

# Bis-Phosphaketenes LM(PCO)<sub>2</sub> (M = Ga, In): A New Class of Reactive Group 13 Metal-Phosphorus Compounds

Mahendra K. Sharma<sup>+, [a]</sup>, Pratima Dhawan<sup>+, [a]</sup>, Christoph Helling,<sup>[a]</sup> Christoph Wölper,<sup>[a]</sup> and Stephan Schulz<sup>\*[a, b]</sup>

**Abstract:** Phosphaketenes are versatile reagents in organo-phosphorus chemistry. We herein report on the synthesis of novel bis-phosphaketenes, LM(PCO)<sub>2</sub> (M = Ga **2a**, In **2b**; L = HC[C(Me)N(Ar)]<sub>2</sub>; Ar = 2,6-*i*-Pr<sub>2</sub>C<sub>6</sub>H<sub>3</sub>) by salt metathesis reactions and their reactions with LGa to metallaphosphenes LGa(OCP)PML (M = Ga **3a**, In **3b**). **3b** represents the first compound with significant In–P  $\pi$ -bonding contribution as was confirmed by DFT calculations. Compounds **3a** and **3b**

selectively activate the N–H and O–H bonds of aniline and phenol at the Ga–P bond and both reactions proceed with a rearrangement of the phosphoethynolate group from Ga–OCP to M–PCO bonding. Compounds **2–5** are fully characterized by heteronuclear (<sup>1</sup>H, <sup>13</sup>C{<sup>1</sup>H}, <sup>31</sup>P{<sup>1</sup>H}) NMR and IR spectroscopy, elemental analysis, and single crystal X-ray diffraction (sc-XRD).

## Introduction

The 2-phosphaethynolate (OCP) anion is widely applied as ligand in *s*-, *p*- and *d*-block element chemistry, in decarbonylation reactions, and as building block for the synthesis of phosphorus-containing compounds, i.e. heterocycles.<sup>[1]</sup> 2-Phosphaethynolate-substituted metal complexes are easily accessible by salt metathesis reactions using Na(OCP)(dioxane)<sub>2.5</sub>. Depending on the electronic nature of the metal center, the OCP anion either binds via the “hard” oxygen or the “soft” phosphorus atom.<sup>[2]</sup> In 2012, the first structurally characterized metallaphosphaketene [Re(PCO)(CO)<sub>2</sub>(triphos)] was reported by Grützmacher *et al.*,<sup>[3a]</sup> followed by the synthesis of a variety of *p*- and *d*-block metal phosphaketenes (Figure 1).<sup>[3–6]</sup> P-bonded main group element and transition metal phosphaketenes are versatile reagents, which can liberate carbon monoxide due to the relatively weak P–CO bond and/or undergo cycloaddition reactions at the P–C double bond.<sup>[3–6]</sup> In remarkable contrast to

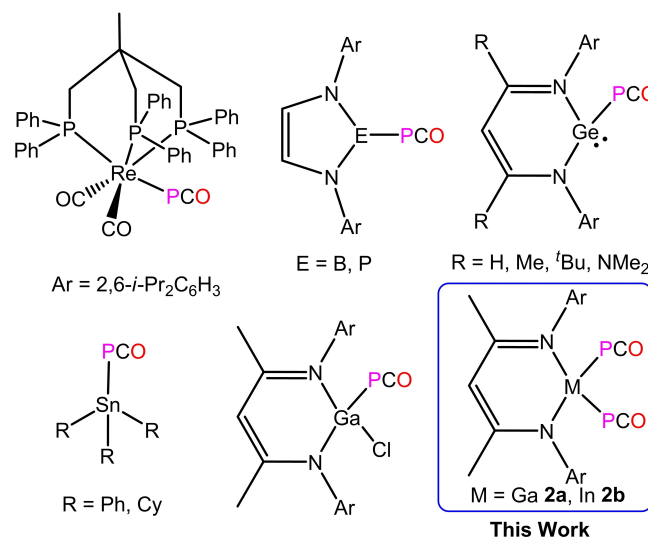


**Figure 1.** Selected *p*- and *d*-block element mono-phosphaketenes and bis-phosphaketenes **2** (this work).

[a] Dr. M. K. Sharma,<sup>+</sup> P. Dhawan,<sup>+</sup> Dr. C. Helling, Dr. C. Wölper, Prof. Dr. S. Schulz  
Institute of Inorganic Chemistry  
University of Duisburg-Essen  
Universitätsstraße 5–7, 45141 Essen (Germany)  
E-mail: stephan.schulz@uni-due.de  
Homepage: [https://www.uni-due.de/ak\\_schulz/index\\_en.php](https://www.uni-due.de/ak_schulz/index_en.php)

[b] Prof. Dr. S. Schulz  
Center for Nanointegration Duisburg-Essen (CENIDE)  
University of Duisburg-Essen  
Carl-Benz-Straße 199, 47057 Duisburg (Germany)

[<sup>+</sup>] These authors contributed equally to this work.

Supporting information for this article is available on the WWW under <https://doi.org/10.1002/chem.202200444>

© 2022 The Authors. Chemistry - A European Journal published by Wiley-VCH GmbH. This is an open access article under the terms of the Creative Commons Attribution Non-Commercial License, which permits use, distribution and reproduction in any medium, provided the original work is properly cited and is not used for commercial purposes.

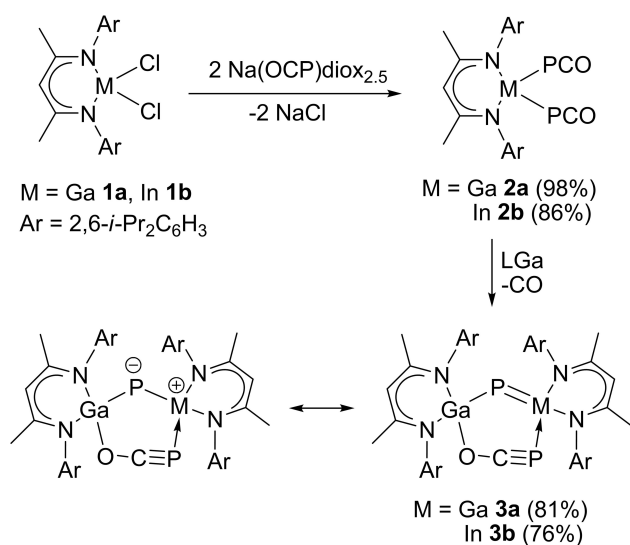
the well-developed chemistry of mono-phosphaketenes, bis-phosphaketenes are unknown, to date, most likely resulting from the high tendency of the PCO groups to undergo cycloaddition reactions, whereas OCP-bonded bis-phosphaethynolato compounds are known.<sup>[7]</sup>

We recently synthesized gallaphosphaketene, LGa(Cl)PCO (L = HC[C(Me)N(Ar)]<sub>2</sub>; Ar = 2,6-*i*-Pr<sub>2</sub>C<sub>6</sub>H<sub>3</sub>) and reported on its reaction with LGa to an unprecedented gallaphosphene LGa(Cl)PGaL,<sup>[8a]</sup> which was found to reversibly react with heteroallenes such as CO<sub>2</sub> and carbodiimides.<sup>[8b]</sup> This remarkable finding and the scarcity of bis-phosphaketenes prompted our interest to bis-phosphaketenes of group 13 metals, and we herein report on the syntheses of two bis-phosphaketenes LM(PCO)<sub>2</sub> (M = Ga **2a**, In **2b**). These were found to react with

LGa to gallaphosphene LGa(OCP)PGaL (**3a**) and indaphosphene LGa(OCP)PGaL (**3b**), which represents the first structurally characterized compound with significant In–P  $\pi$ -bonding contribution. The promising potential of **3a** and **3b** in N–H and O–H bond activation reactions is also reported.

## Results and Discussion

Salt elimination reactions of LGaCl<sub>2</sub> (**1a**) and LInCl<sub>2</sub> (**1b**)<sup>[9]</sup> with two equivalents of Na(OCP)(dioxane)<sub>2.5</sub> yielded the corresponding bis-phosphaketenes LGa(PCO)<sub>2</sub> (**2a**) and LIn(PCO)<sub>2</sub> (**2b**) as pale yellow crystalline solids in high yields (>86%, Scheme 1). Compounds **2a** and **2b** are soluble in common organic solvents and stable under an inert gas atmosphere at ambient temperature in both solution and solid state for weeks. The <sup>1</sup>H NMR



**Scheme 1.** Synthesis of bis-phosphaketenes **2** and their reactions with LGa to compounds **3**.

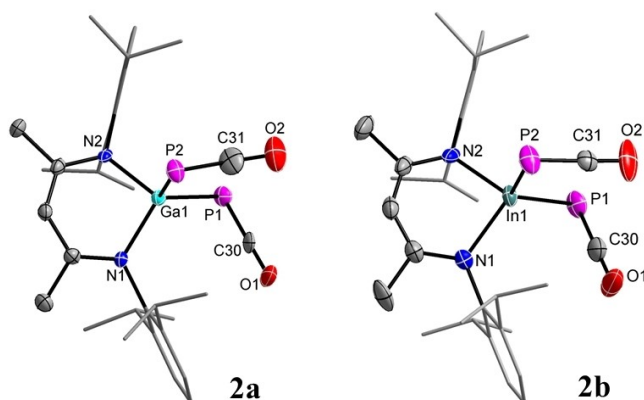


**Figure 2.** Molecular structures of bis-phosphaketenes **2a** and **2b**. Ellipsoids set at 50% probability; hydrogen atoms and alternate positions of the disordered parts are omitted for clarity. Selected bond lengths (Å) and angles (°): **2a**: Ga1–P1 2.327(2), Ga1–P2 2.346(3); P1–Ga1–P2 118.14(10). **2b**: In1–P1 2.485(4), In1–P2 2.530(5); P1–In1–P2 119.52(19).

spectra of **2a** and **2b** each exhibit one set of resonances for the aryl (Ar) groups of the  $\beta$ -diketiminato ligand, indicating a symmetric nature of the molecules in solution (Table S1). <sup>13</sup>C{<sup>1</sup>H} NMR spectra of **2a** (183.6 ppm, <sup>1</sup>J<sub>CP</sub> = 98.2 Hz) and **2b** (181.0 ppm, <sup>1</sup>J<sub>CP</sub> = 105.8 Hz) show the expected doublets for the phosphaketonyl carbon atoms, whereas the <sup>31</sup>P{<sup>1</sup>H} NMR spectra display sharp singlets at –356.0 ppm (**2a**) and –375.8 ppm (**2b**), respectively, which are in a typical region of mono-phosphaketenes (–354.9 to –394.6 ppm).<sup>[3–6]</sup> The IR spectra of **2a** (1934, 1907 cm<sup>–1</sup>) and **2b** (1918, 1894 cm<sup>–1</sup>) each show two strong absorption bands for the PCO stretching vibrations most likely due to the symmetrical and unsymmetrical stretches, which are in a comparable range to that observed for mono-phosphaketene LGa(Cl)PCO (1910 cm<sup>–1</sup>).<sup>[8a]</sup> To the best of our knowledge, compounds **2a** and **2b** are the first metal bis-phosphaketenes reported, to date.

The solid-state molecular structures of compounds **2a** and **2b** were determined by sc-XRD (Figure 2). The compounds crystallize in the orthorhombic space groups *P2<sub>1</sub>2<sub>1</sub>2<sub>1</sub>* (**2a**) and *Pna2<sub>1</sub>* (**2b**), respectively.<sup>[10]</sup> The Ga and In atoms are four-coordinate and adopt distorted tetrahedral geometries and the PCO units are almost linear (174.2(8), 176.7(13)° **2a**; 176.0(2), 178.0(2)° **2b**) as is typical for metal phosphaketenes. The solid-state structures reveal that the PCO groups are not equal since one resides almost parallel to the C<sub>3</sub>N<sub>2</sub>M (M = Ga **2a**, In **2b**) plane, while the other is perpendicular to this plane.

The almost equidistant Ga1–P1 (2.327(2) Å) and Ga1–P2 (2.346(3) Å) bonds in **2a** agree with sum of the calculated single-bond radii (Ga 1.24 Å; P 1.11 Å),<sup>[11]</sup> and experimentally observed Ga–P single bond lengths in LGa(O<sub>3</sub>SCF<sub>3</sub>)(PPh<sub>2</sub>) (2.312(3) Å),<sup>[12a]</sup> LGa(P<sub>4</sub>) (2.340(2), 2.346(2) Å),<sup>[12b]</sup> and LGa(H)(PPh<sub>2</sub>) (2.363(1) Å).<sup>[12c]</sup> The In1–P1 (2.485(4) Å) bond in compound **2b** is slightly shorter than the In1–P2 (2.530(5) Å) bond, which agrees with the sum of the calculated single-bond radii (In 1.42 Å; P 1.11 Å)<sup>[11]</sup> and In–P single bonds in [(2,4,6-*t*-Bu<sub>3</sub>C<sub>6</sub>H<sub>2</sub>)In-PSit-Bu<sub>3</sub>]<sub>2</sub> (2.515(2), 2.503(2) Å),<sup>[13a]</sup> and [In<sub>3</sub>(In<sub>2</sub>)<sub>3</sub>(PhP)<sub>4</sub>(Ph<sub>2</sub>P<sub>2</sub>)<sub>3</sub>Cl<sub>7</sub>(PET<sub>3</sub>)<sub>3</sub>] (2.53–2.61 Å), respectively.<sup>[13b]</sup>

Reactions of compounds **2a** and **2b** with equimolar amounts of LGa yielded metallaphosphenes L(OCP)GaPGaL (**3a**) and L(OCP)GaPInL (**3b**) as orange crystalline solids (Scheme 1). Compound **3a** was previously prepared by a different synthetic route reacting gallaphosphene LGa(Cl)PGaL with Na(OCP)(dioxane)<sub>2.5</sub>,<sup>[8a]</sup> while compound **3b** represents the first compound with In–P  $\pi$ -bonding contribution. Interestingly, upon reaction of **2b** with LGa, the In–PCO bond rearranges to a Ga–OCP bond in **3b**, while the phosphorus datively coordinates to the indium atom. A comparable structural motif was previously observed for **3a**.<sup>[8a]</sup> Compound **3b** is sparingly soluble in organic solvents and stable under an inert gas atmosphere at ambient temperature in both solution and solid state, but it decomposes rapidly when exposed to air. <sup>1</sup>H and <sup>13</sup>C{<sup>1</sup>H} NMR spectra of **3b** show two distinct sets of signals for the inequivalent  $\beta$ -diketiminato ligands at ambient temperature, and the <sup>31</sup>P{<sup>1</sup>H} NMR spectrum of **3a** (–290.5, –320.8 ppm) and **3b** (–313.1, –333.1 ppm) show two singlets, which are shifted to higher field compared to the phosphaketenes (**2a** –356.0; **2b** –375.8 ppm), respectively. The <sup>1</sup>J<sub>CP</sub>

coupling constant in **3a** (40.1 Hz) and **3b** (48.1 Hz) are far smaller than those observed in **2** (98.2 Hz **2a**; 105.8 Hz **2b**) and other *p*-block element phosphaketenes (85.4–101.0 Hz).<sup>[4–6]</sup> These small  $^1J_{CP}$  coupling constants indicate a phosphoethynolate (–OCP) bonding in **3a** and **3b** rather than the phosphaketene (–PCO) bonding due to a greater contribution of the P 3 *s* orbital to the C–P bond in the latter.<sup>[1b]</sup> The IR spectra of **3a** and **3b** confirmed the phosphoethynolate binding with strong –OCP asymmetric stretches at 1739 and 1729  $\text{cm}^{-1}$ , respectively, which are comparable to that of Na(OCP)(dioxane)<sub>2.5</sub> ( $\nu(\text{C}\equiv\text{P}) = 1755 \text{ cm}^{-1}$ ).<sup>[14]</sup> Unfortunately, we were unable to assign the O–C stretches because of the overlapping region of C–N/C stretches of the ligand L. Variable temperature (VT)  $^1\text{H}$  NMR spectra (Figures S37, S38) revealed that **3a** and **3b** are stable in solution up to 100 °C. Moreover, they also show remarkable stability in the solid state ( $T_d = 127 \text{ °C}$  for **3a**, 176 °C for **3b**).

The molecular structure of compound **3b** in the solid state was determined by sc-XRD, further confirming the Ga–OCP binding mode of the phosphoethynolate substituent (Figure 3).<sup>[10]</sup> Compound **3b** crystallizes in the orthorhombic space group *Pbca*. The OCP unit in **3b** binds via the oxygen atom (O1) to the gallium atom (Ga1), while the indium atom (In1) is datively coordinated by the phosphorus atom P2. This finding is consistent with the HSAB principle, according to which the “hard” Ga atom prefers binding to the oxygen atom and the rather “soft” In atom prefers P-coordination. The In and Ga atoms in compound **3b** are both four-coordinate and adopt distorted tetrahedral geometries as was previously observed in **3a**.<sup>[8a]</sup> The In1–P1–Ga1 bond angle in compound **3b** (98.09(4)°) is slightly smaller than the Ga1–P1–Ga2 bond angle reported for **3a** (99.86(7)°),<sup>[8a]</sup> however, considering the rotational disorder of the central P(OCP) moiety between the two gallium atoms in **3a**, the difference is likely insignificant. The In1–P1 (2.3813(12) Å) bond length in **3b** perfectly agrees with sum of the calculated In–P double bond radii (In 1.36 Å; P 1.02 Å),<sup>[15]</sup> however, the short Ga1–P1 (2.2370(12) Å) bond points toward a partly delocalized  $\pi$ -electron system within the In–P–Ga unit.

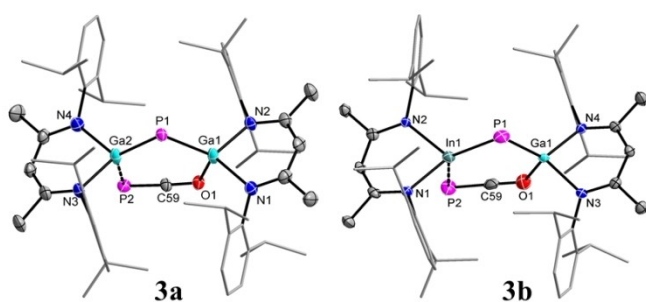
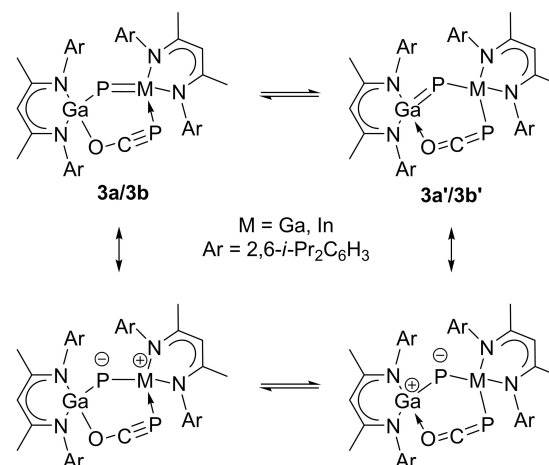


**Figure 3.** Molecular structures of compounds **3a**<sup>[8a]</sup> and **3b**. Ellipsoids set at 50% probability; hydrogen atoms and alternate positions of the disordered parts (in **3a**) are omitted for clarity. Selected bond lengths (Å) and angles (°): **3a**: Ga1–P1 2.2943(16), Ga2–P1 2.297(2), Ga1–O1 1.977(4), O1–C59 1.223(7), C59–P2 1.592(6), Ga2–P2 2.4798(16); Ga1–P1–Ga2 99.86(7), O1–C59–P2 176.9(7). **3b**: In1–P1 2.3813(12), Ga1–P1 2.2370(12), In1–P2 2.7177(12), P2–C59 1.609(5), O1–C59 1.204(5), Ga1–O1 2.054(3); P1–In1–P2 125.60(4), O1–C59–P2 177.7(4).

The –OCP binding mode leads to a rather short Ga1–O1 bond (2.054(3) Å) and a long In1–P2 bond (2.7177(12) Å), which is close to the mean In–P bond distance of 2.64(10) Å reported in the CSD.<sup>[16]</sup>

To gain a deeper understanding of the electronic structures of **3a** and **3b**, DFT calculations were performed. Geometry optimizations of **3a** and **3b** gave two minima for both compounds, one of which corresponds to the phosphoethynolate isomers observed by sc-XRD, LGa(OCP)PML (M = Ga **3a**, In **3b**), while the second are represented by the corresponding phosphaketenyl isomers, LGaP(OCP)ML (M = Ga **3a'**, In **3b'**), respectively (Figure S46). The phosphoethynolate isomers, **3a** and **3b**, are both slightly more stable by 3.6 kcal mol<sup>−1</sup> (M = Ga) and 0.7 kcal mol<sup>−1</sup> (M = In), respectively. However, the small energy differences and slight geometric changes between both isomers suggest that both structures can co-exist in solution (Scheme 2), which is consistent with the observed reactivity (see below). Variable-temperature (VT)  $^1\text{H}$  NMR spectroscopy studies with **3a** and **3b** did not allow freezing the equilibrium, indicating a very small activation barrier for the interconversion.

The HOMOs of **3a** and **3b** are reflected by the phosphorus-centered electron lone pairs (Figures 4, S47, S48), which are of pure *p*-orbital character (**3a** 99.4% *p*, **3b** 99.3% *p*) according to NBO analysis. In addition, electron lone pairs at the central P atom with high *s*-orbital character (**3a** 66.8% *s*, 33.0% *p*



**Scheme 2.** Proposed equilibrium and resonance structures of **3a** and **3b**.

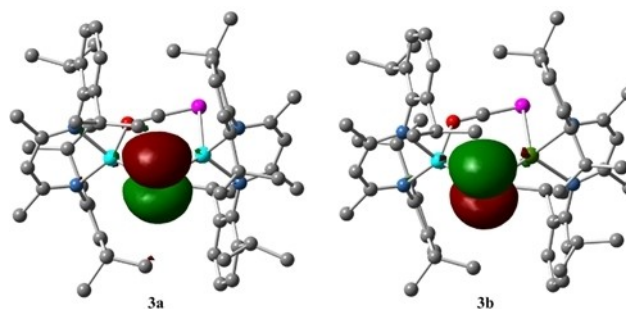
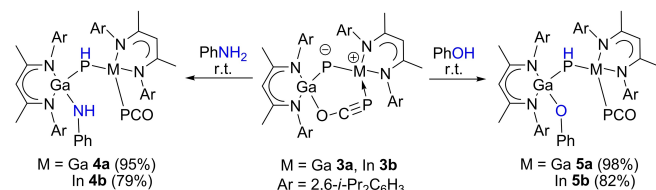


**Figure 4.** HOMOs of **3a** and **3b**. Hydrogen atoms are omitted for clarity.

(HOMO-2); **3b** 74.7% s, 25.1% p (HOMO-3)) were also found. Second order perturbation theory (SOPT) analysis disclosed strong additional  $\pi$ -type interactions of both phosphorus electron lone pairs with the antibonding  $\sigma^*(M-N)$  orbitals of the LM fragments accounting to  $72.3 \text{ kcal mol}^{-1}$  ( $s(P) \rightarrow \sigma^*(Ga-N)$ ) and  $56.2 \text{ kcal mol}^{-1}$  ( $p(P) \rightarrow \sigma^*(Ga-N)$ ) for **3a**. In **3b** the P $\rightarrow$ M backdonation is slightly stronger to the Ga center ( $s(P) \rightarrow \sigma^*(Ga-N)$   $31.7 \text{ kcal mol}^{-1}$ ,  $p(P) \rightarrow \sigma^*(Ga-N)$   $26.4 \text{ kcal mol}^{-1}$ ) than to the In center ( $s(P) \rightarrow \sigma^*(In-N)$   $31.8 \text{ kcal mol}^{-1}$ ,  $p(P) \rightarrow \sigma^*(In-N)$   $15.0 \text{ kcal mol}^{-1}$ ), respectively. The P–M  $\pi$  interactions thus result in increased Wiberg bond indices (WBI; **3a** Ga–P 1.13, 1.14; **3b** Ga–P 1.16, In–P 0.97) and Mayer Bond Orders (MBO; **3a** Ga–P 1.31, 1.38; **3b** Ga–P 1.37, In–P 1.28), as observed for other gallapnictenes.<sup>[17,8a]</sup> However, these values suggest less strongly localized M–P single and double bonds in **3a** and **3b** compared to L(Cl)GaPGaL.<sup>[8a]</sup> The WBIs between the Ga and In centers and the PCO unit (**3a** Ga–P 0.41, Ga–O 0.19; **3b** In–P 0.31, Ga–O 0.19) rather suggest ionic/electrostatic interactions, while three P–C bonds and one C–O bond were found within the PCO unit, consistent with the phosphoethynolate bonding mode of the PCO moiety. Considering the NBO analyses of isomers **3a'** and **3b'**, only slight alterations in the bonding were observed, as the WBIs (**3a'** Ga–P 1.07, 1.18; **3b'** Ga–P 1.20, In–P 0.95) and MBOs (**3a'** Ga–P 1.22, 1.43; **3b'** Ga–P 1.39, In–P 1.21) within the central MPGa units are comparable to those of **3a** and **3b**, respectively. Similarly, the  $\pi$ -type P–M interactions in the PCO-bonded isomers **3a'** ( $s(P) \rightarrow \sigma^*(Ga-N)$   $72.4 \text{ kcal mol}^{-1}$ ;  $p(P) \rightarrow \sigma^*(Ga-N)$   $56.6 \text{ kcal mol}^{-1}$ ) and **3b'** ( $s(P) \rightarrow \sigma^*(Ga-N)$   $35.0 \text{ kcal mol}^{-1}$ ;  $p(P) \rightarrow \sigma^*(Ga-N)$   $29.0 \text{ kcal mol}^{-1}$ ;  $s(P) \rightarrow \sigma^*(In-N)$   $32.7 \text{ kcal mol}^{-1}$ ;  $p(P) \rightarrow \sigma^*(In-N)$   $15.3 \text{ kcal mol}^{-1}$ ) disclosed by SOPT analyses are comparable to those of the OCP-bonded isomers **3a** and **3b**, respectively.

Low-valent main group element compounds have attracted enormous interest in the activation of polar and non-polar X–H bonds (X=H, O, N, C, etc.) of small molecules including the development of catalytic reactions similar to those of transition metal compounds.<sup>[18]</sup> We recently expanded such studies to gallaphosphene L(Cl)GaPGaL, demonstrating that polar X–H bonds are readily activated via 1,2 addition to the Ga–P double bond.<sup>[19]</sup> We therefore probed the reactivity of **3a** and **3b** toward X–H bond activation and reacted compounds **3a** and **3b** with equimolar amounts of aniline in toluene at ambient temperature, immediately resulting in N–H bond activation and formation of **4a** and **4b**, respectively. Analogous reactions with phenol gave the O–H bond activation products **5a** and **5b** in almost quantitative yields (Scheme 3).



**Scheme 3.** Reactions of compounds **3a** and **3b** with aniline and phenol to the corresponding N–H and O–H bond activation products.

Compounds **4** and **5** are colorless crystalline solids, which are soluble in common organic solvents and stable under an inert gas atmosphere at ambient temperature in both solution and solid state. The <sup>1</sup>H NMR spectra of compounds **4** and **5** exhibit two sets of signals for the Ar groups of the  $\beta$ -diketiminate ligand as was previously reported for LGa-substituted gallapnictenes,<sup>[17]</sup> dipnictanes,<sup>[20]</sup> dipnictenes,<sup>[21]</sup> and other complexes.<sup>[22,23]</sup> The <sup>13</sup>C{<sup>1</sup>H} NMR spectra of **4a** (185.9 ppm, <sup>1</sup>J<sub>PC</sub> = 96.5 Hz), **4b** (183.8 ppm, <sup>1</sup>J<sub>PC</sub> = 102.7 Hz), **5a** (188.0 ppm, <sup>1</sup>J<sub>PC</sub> = 94.6 Hz), and **5b** (185.4 ppm, <sup>1</sup>J<sub>PC</sub> = 101.9 Hz) each exhibit the expected doublet due to the PCO carbon atom. The <sup>1</sup>J<sub>PC</sub> coupling constants compare well with those of the phosphaketenes<sup>[3–6]</sup> but are larger than those of **3a** (<sup>1</sup>J<sub>PC</sub> = 40.1 Hz) and **3b** (<sup>1</sup>J<sub>PC</sub> = 48.1 Hz), respectively, suggesting a switch in coordination of the phosphoethynolate substituents from –OCP to –PCO in compounds **4** and **5**. Base induced –OCP to –PCO coordination switching was previously reported by Grützmacher and Goicoechea *et al.*<sup>[4b,24]</sup> The <sup>31</sup>P{<sup>1</sup>H} NMR spectra of **4a** (–291.1, –363.8 ppm), **4b** (–314.7, –373.3 ppm), **5a** (–296.1, –362.5 ppm), and **5b** (–322.6, –371.9 ppm) each showed two sharp singlets, which are shifted to lower field than those of the starting compounds **3a** (–290.5, –320.8 ppm) and **3b** (–313.1, –333.1 ppm). However, the latter resonances in **4** and **5** are similar to those observed for phosphaketenes<sup>[3–6]</sup> and support the switch in coordination of the phosphoethynolate substituent. The proton coupled <sup>31</sup>P NMR spectra of **4a** (–291.1 ppm, <sup>1</sup>J<sub>PH</sub> = 176.9 Hz), **4b** (–314.7 ppm, <sup>1</sup>J<sub>PH</sub> = 162.8 Hz), **5a** (–296.1 ppm, <sup>1</sup>J<sub>PH</sub> = 173.9 Hz), and **5b** (–322.6 ppm, <sup>1</sup>J<sub>PH</sub> = 163.1 Hz) each display a doublet for the P–H units, and the coupling constants agree with the <sup>1</sup>J<sub>PH</sub> coupling constants observed for the 1,2 addition products of reagents containing X–H bonds (X=C, N, O etc.) to gallaphosphene LGa(Cl)PGaL (<sup>1</sup>J<sub>PH</sub> = 178.9–181.0 Hz).<sup>[8a,b]</sup>

The solid-state molecular structures of compounds **4a** (Figure 5), **4b** (Figure 5), and **5b** (Figure S45) were determined by sc-XRD. All compounds crystallize in the monoclinic space group C2/c, and the structures confirmed the –PCO bonding mode of the phosphaketene substituents.<sup>[10]</sup>

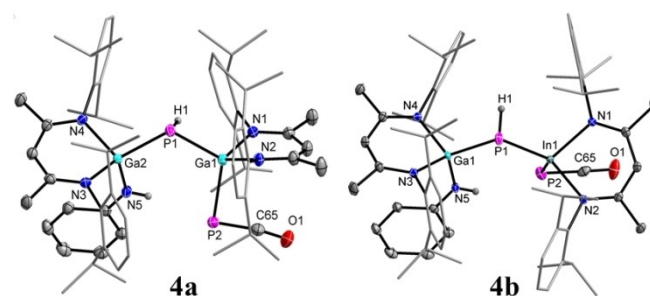


**Figure 5.** Molecular structures of compounds **4a** and **4b**. Ellipsoids set at 50% probability; hydrogen atoms, solvent molecules (benzene in **4a**, and toluene in **4b**), and alternate positions of the disordered parts are omitted for clarity. Selected bond lengths (Å) and angles (°): **4a**: Ga1–P1 2.3396(6), Ga1–P2 2.3859(6), Ga2–N3 1.9803(18), Ga2–P1 2.3369(6); Ga2–P1–Ga1 113.14(2). **4b**: In1–P1 2.4887(4), In1–P2 2.5447(5), Ga1–N5 1.8771(10), Ga1–P1 2.3230(4); Ga1–P1–In1 108.646(17).



The four-coordinate Ga/In atoms adopt distorted tetrahedral geometries and the P atoms trigonal pyramidal geometries. The Ga1–P1–Ga2 bond angle in **4a** (113.14(2)°) is comparable to that observed for LGa(Cl) PH(OC(Ph) CH<sub>2</sub>)GaL (116.8(2)°),<sup>[8a]</sup> but much larger than that of **3a** (99.86(7)°).<sup>[8a]</sup> The Ga1–P1 (2.3396(6) Å) and Ga2–P1 (2.3369(6) Å) bond lengths are equidistant and compare well with the Ga–P single bond lengths mentioned previously.<sup>[12]</sup> Interestingly, the molecular structures of compounds **4b** and **5b** confirm the selective addition of the N–H and O–H bonds to the Ga1–P1 bond rather than to the In1–P1 double bond in **3b**, which is most likely caused by the higher nitro- and oxophilicity of gallium than indium. The In1–P1 bond lengths in **4b** (2.4887(4) Å) and **5b** (2.4896(10) Å) are consistent with the In–P single bonds<sup>[13]</sup> and agree with the calculated In–P single bond radii (In 1.42 Å; P 1.11 Å),<sup>[11]</sup> whereas they are significantly elongated compared to the corresponding In–P double bond **3b** (2.3813(12) Å). Similarly, the Ga1–P1 bond lengths in **4b** (2.3230(4) Å) and **5b** (2.3085(10) Å) agree with experimental<sup>[12]</sup> and calculated<sup>[11]</sup> Ga–P single bond lengths, and the In1–P2 bond lengths in **4b** (2.5447(5) Å) and **5b** (2.5273(11) Å) are comparable to the In–P single bond lengths.

## Conclusion

In summary, the syntheses and single crystal X-ray structures of the first bis-phosphaketenes **2a** and **2b** and their reactions with LGa to –OCP coordinated metallaphosphenes **3a** and **3b** is reported. Even though the  $\pi$ -electron system in **3a** and **3b** is rather delocalized within the M–P–Ga units (M = Ga, In), compound **3b** represents the first structurally characterized compound with a substantial In–P  $\pi$ -bonding contribution. Compounds **3a** and **3b** are promising starting reagents for the activation of polar X–H bonds as was shown in reactions with aniline and phenol, which selectively occurred at the Ga–P bond with formation of compounds **4** and **5**.

## Supporting Information

Supporting Information Available: Detailed synthetic procedures and analytical data (<sup>1</sup>H, <sup>13</sup>C, <sup>31</sup>P NMR and IR spectra) of **1–5**, plots of DFT calculated optimized geometries and coordinates, WBI and NBO charges as well as selected molecular orbitals of **3a** and **3b**, and cif files of **2–5**.

Deposition Number(s) 2038995 (for **2a**), 2132670 (for **2b**), 2038997 (for **3a**), 2132671 (for **3b**), 2132672 (for **4a**), 2132673 (for **4b**), and 2132674 (for **5b**) contain(s) the supplementary crystallographic data for this paper. These data are provided free of charge by the joint Cambridge Crystallographic Data Centre and Fachinformationszentrum Karlsruhe Access Structures service.

## Acknowledgements

Financial support from the Deutsche Forschungsgemeinschaft (SCHU 1069/27-1), Evonik Industries (C.H.) and the University of Duisburg-Essen (S.S.) is gratefully acknowledged. Open Access funding enabled and organized by Projekt DEAL.

## Conflict of Interest

The authors declare no conflict of interest.

## Data Availability Statement

The data that support the findings of this study are available in the supplementary material of this article.

**Keywords:** bond activation · double bonds · gallium · indium · main-group elements · phosphorus

- [1] a) X. Chen, S. Alidori, F. F. Puschmann, G. Santiso-Quinones, Z. Benkő, Z. Li, G. Becker, H.-F. Grützmacher, H. Grützmacher, *Angew. Chem. Int. Ed.* **2014**, *53*, 1641–1645; *Angew. Chem.* **2014**, *126*, 1667–1671; b) J. M. Goicoechea, H. Grützmacher, *Angew. Chem. Int. Ed.* **2018**, *57*, 16968–16994; *Angew. Chem.* **2018**, *130*, 17214–17240; c) L. Weber, *Eur. J. Inorg. Chem.* **2018**, 2175–2227.
- [2] D. Heift, Z. Benkő, H. Grützmacher, *Dalton Trans.* **2014**, *43*, 5920–5928.
- [3] **Transition metal phosphaketenes:** a) S. Alidori, D. Heift, G. Santiso-Quinones, Z. B. H. Grützmacher, M. Caporali, L. Gonsalvi, A. Rossin, M. Peruzzini, *Chem. Eur. J.* **2012**, *18*, 14805–14811; b) L. Liu, D. A. Ruiz, F. Dahcheh, G. Bertrand, R. Suter, A. M. Tondreauc, H. Grützmacher, *Chem. Sci.* **2016**, *7*, 2335–2341; c) A. R. Jupp, M. B. Geeson, J. E. McGrady, J. M. Goicoechea, *Eur. J. Inorg. Chem.* **2016**, 639–648; d) L. N. Grant, J. Krzystek, B. Pinter, J. Telsler, H. Grützmacher, D. J. Mindiola, *Chem. Commun.* **2019**, *55*, 5966–5969.
- [4] **Group 13 element phosphaketenes:** a) S. Hagspiel, F. Fantuzzi, R. D. Dewhurst, A. Gärtner, F. Lindl, A. Lamprecht, H. Braunschweig, *Angew. Chem. Int. Ed.* **2021**, *60*, 13666–13670; *Angew. Chem.* **2021**, *133*, 13780–13784; b) D. W. N. Wilson, M. P. Franco, W. K. Myers, J. E. McGrady, J. M. Goicoechea, *Chem. Sci.* **2020**, *11*, 862–869; c) W. Yang, K. E. Krantz, D. A. Dickie, A. Molino, D. J. D. Wilson, R. J. Gilliard, *Angew. Chem. Int. Ed.* **2020**, *59*, 3971–3975; *Angew. Chem.* **2020**, *132*, 3999–4003; d) D. Wilson, W. Myers, J. M. Goicoechea, *Dalton Trans.* **2020**, *49*, 15249–15255; e) Y. Mei, J. E. Borger, D. J. Wu, H. Grützmacher, *Dalton Trans.* **2019**, *48*, 4370–4374.
- [5] **Group 14 element phosphaketenes:** a) N. Del Rio, A. Baceiredo, N. Saffon-Merceron, D. Hashizume, D. Lutters, T. Müller, T. Kato, *Angew. Chem. Int. Ed.* **2016**, *55*, 4753–4758; *Angew. Chem.* **2016**, *128*, 4831–4836; b) S. Yao, Y. Xiong, T. Szilvási, H. Grützmacher, M. Driess, *Angew. Chem. Int. Ed.* **2016**, *55*, 4781–4785; *Angew. Chem.* **2016**, *128*, 4859–4863; c) Y. Wu, L. Liu, J. Su, J. Zhu, Z. Ji, Y. Zhao, *Organometallics* **2016**, *35*, 1593–1596; d) Y. Xiong, S. Yao, T. Szilvási, E. Ballester-Martinez, H. Grützmacher, M. Driess, *Angew. Chem. Int. Ed.* **2017**, *56*, 4333–4336; *Angew. Chem.* **2017**, *129*, 4397–4400; e) A. Hinz, J. M. Goicoechea, *Chem. Eur. J.* **2018**, *24*, 7358–7363; f) D. Heift, Z. Benkő, H. Grützmacher, *Chem. Eur. J.* **2014**, *20*, 11326–11330; g) A. Hinz, J. M. Goicoechea, *Dalton Trans.* **2018**, *47*, 8879–8883; h) S. Bestgen, M. Mehta, T. C. Johnstone, P. W. Roesky, J. M. Goicoechea, *Chem. Eur. J.* **2020**, *26*, 9024–9031; i) D. C. H. Do, A. V. Protchenko, P. Vasko, J. Campos, E. L. Kolychev, S. Aldridge, *Z. Anorg. Allg. Chem.* **2018**, *644*, 1238–1242.
- [6] **Group 15 element phosphaketenes:** a) M. Mehta, J. E. McGrady, J. M. Goicoechea, *Chem. Eur. J.* **2019**, *25*, 5445–5450; b) Z. Li, X. Chen, M. Bergeler, M. Reiher, C. Y. Su, H. Grützmacher, *Dalton Trans.* **2015**, *44*, 6431–6438; c) L. Liu, D. A. Ruiz, D. Munz, G. Bertrand, *Chem* **2016**, *1*, 147–153; d) M. M. Hansmann, D. A. Ruiz, L. Liu, R. Jazzar, G. Bertrand, *Chem. Sci.* **2017**, *8*, 3720–3725; e) J. E. Walley, L. S. Warring, E. Kertész, G.

- Wang, D. A. Dickie, Z. Benkó, R. J. Gilliard, *Inorg. Chem.* **2021**, *60*, 4733–4743.
- [7] a) R. J. Gilliard Jr., D. Heift, Z. Benko, J. M. Keiser, A. L. Rheingold, H. Grützmacher, J. D. Protasiewicz, *Dalton Trans.* **2018**, *47*, 666–669; b) A. D. Obi, H. R. Machost, D. A. Dickie, R. J. Gilliard, Jr., *Inorg. Chem.* **2021**, *60*, 12481–12488.
- [8] a) M. K. Sharma, C. Wölper, G. Haberhauer, S. Schulz, *Angew. Chem. Int. Ed.* **2021**, *60*, 6784–6790; *Angew. Chem.* **2021**, *133*, 6859–6865; b) M. K. Sharma, C. Wölper, G. Haberhauer, S. Schulz, *Angew. Chem. Int. Ed.* **2021**, *60*, 21784–21788; *Angew. Chem.* **2021**, *40*, 21953–21957.
- [9] M. Stender, B. E. Eichler, N. J. Hardman, P. P. Power, J. Prust, M. Noltemeyer, H. W. Roesky, *Inorg. Chem.* **2001**, *40*, 2794–2799.
- [10] Full crystallographic data of all structurally characterized compounds described herein as well as central bond lengths and angles (Tables S2–S3 and Figures S39–S45) are given in the Supporting Information.
- [11] P. Pyykkö, M. Atsumi, *Chem. Eur. J.* **2009**, *15*, 186–197.
- [12] a) N. Burford, P. J. Ragona, K. N. Robertson, T. S. Cameron, N. J. Hardman, P. P. Power, *J. Am. Chem. Soc.* **2002**, *124*, 382–383; b) G. Prabusankar, A. Doddi, C. Gemel, M. Winter, R. A. Fischer, *Inorg. Chem.* **2010**, *49*, 7976–7980; c) A. Seifert, D. Scheid, G. Linti, T. Zessin, *Chem. Eur. J.* **2009**, *15*, 12114–12120.
- [13] a) T. Rotter, A. N. Kneifel, P. Mayer, M. Westerhausen, *Inorg. Chem. Commun.* **2005**, *8*, 809–812; b) C. von Hänisch, D. Fenske, M. Kattannek, R. Ahlrichs, *Angew. Chem. Int. Ed.* **1999**, *38*, 2736–2738; *Angew. Chem.* **1999**, *111*, 2900–2902.
- [14] F. F. Puschmann, D. Stein, D. Heift, C. Hendriksen, Z. A. Gal, H. F. Grützmacher, H. Grützmacher, *Angew. Chem. Int. Ed.* **2011**, *50*, 8420–8423; *Angew. Chem.* **2011**, *123*, 8570–8574.
- [15] P. Pyykkö, M. Atsumi, *Chem. Eur. J.* **2009**, *15*, 12770–12779.
- [16] A CSD-search for P–In single bonds yielded 158 hits (459 bonds) ranging from 2.48 to 3.055 Å (mean bond length is 2.64(10) Å). Five compounds with bond distances above 3.1 Å were excluded. Cambridge Structural Database, Version 5.41 Update 3 (Aug 2021); see also: F. H. Allen, *Acta Cryst.* **2002**, *58*, 380–388.
- [17] a) C. Ganesamoorthy, C. Helling, C. Wölper, W. Frank, E. Bill, G. E. Cutsail III, S. Schulz, *Nat. Commun.* **2018**, *9*, 87–95; b) C. Helling, C. Wölper, S. Schulz, *J. Am. Chem. Soc.* **2018**, *140*, 5053–5056; c) J. Krüger, C. Ganesamoorthy, L. John, C. Wölper, S. Schulz, *Chem. Eur. J.* **2018**, *24*, 9157–9164; d) C. Helling, C. Wölper, Y. Schulte, G. Cutsail III, S. Schulz, *Inorg. Chem.* **2019**, *58*, 10323–10332; e) J. Schoening, L. John, C. Wölper, S. Schulz, *Dalton Trans.* **2019**, *48*, 17729–17734.
- [18] a) P. P. Power, *Nature* **2010**, *463*, 171–177; b) C. Weetman, S. Inoue, *ChemCatChem* **2018**, *10*, 4213–4228; c) R. L. Melen, *Science* **2019**, *363*, 479–484; d) C. Weetman, *Chem. Eur. J.* **2021**, *27*, 1941–1954; e) T. J. Hadlington, M. Driess, C. Jones, *Chem. Soc. Rev.* **2018**, *47*, 4176–4197; f) D. W. Stephan, *Science* **2016**, *354*, 6317.
- [19] M. K. Sharma, C. Wölper, S. Schulz, *Dalton Trans.* **2022**, *51*, 1612–1616.
- [20] C. Helling, C. Wölper, S. Schulz, *Eur. J. Inorg. Chem.* **2020**, 4225–4235.
- [21] a) L. Song, J. Schoening, C. Wölper, S. Schulz, P. R. Schreiner, *Organometallics* **2019**, *38*, 1640–1647; b) J. Krüger, J. Schoening, C. Ganesamoorthy, L. John, C. Wölper, S. Schulz, *Z. Anorg. Allg. Chem.* **2018**, *644*, 1028–1033; c) L. Tuscher, C. Helling, C. Wölper, W. Frank, A. S. Nizovtsev, S. Schulz, *Chem. Eur. J.* **2018**, *24*, 3241–3250.
- [22] a) J. Krüger, C. Wölper, S. Schulz, *Inorg. Chem.* **2020**, *59*, 11142–11151; b) C. Helling, C. Wölper, G. E. Cutsail III, G. Haberhauer, S. Schulz, *Chem. Eur. J.* **2020**, *26*, 13390–13399; c) C. Helling, G. E. Cutsail III, H. Weinert, C. Wölper, S. Schulz, *Angew. Chem. Int. Ed.* **2020**, *59*, 7561–7568; *Angew. Chem.* **2020**, *132*, 7631–7638.
- [23] a) J. Krüger, C. Wölper, L. John, L. Song, P. R. Schreiner, S. Schulz, *Eur. J. Inorg. Chem.* **2019**, 1669–1678; b) L. Tuscher, C. Helling, C. Ganesamoorthy, J. Krüger, C. Wölper, W. Frank, A. S. Nizovtsev, S. Schulz, *Chem. Eur. J.* **2017**, *23*, 12297–12304; c) C. Ganesamoorthy, J. Krüger, C. Wölper, A. S. Nizovtsev, S. Schulz, *Chem. Eur. J.* **2017**, *23*, 2461–2468; d) L. Tuscher, C. Ganesamoorthy, D. Bläser, C. Wölper, S. Schulz, *Angew. Chem.* **2015**, *127*, 10803–10807; *Angew. Chem. Int. Ed.* **2015**, *54*, 10657–10661.
- [24] a) Z. Li, X. Chen, Z. Benkó, L. Liu, D. A. Ruiz, J. L. Peltier, G. Bertrand, C.-Y. Su, H. Grützmacher, *Angew. Chem. Int. Ed.* **2016**, *55*, 6018–6022; *Angew. Chem.* **2016**, *128*, 6122–6126.

Manuscript received: February 2, 2022

Accepted manuscript online: February 28, 2022

Version of record online: March 14, 2022